GOODRICK

18 JUN 1982

(1)

DEVELOPMENT OF METHODS FOR ASSESSMENT OF GLIDING PARACHUTE APPLICATIONS

THOMAS F. GOODRICK
US ARMY NATICK R&D LABORATORIES
NATICK, MASSACHUSETTS 01760

In order to assess the possible utility of gliding parachutes, it was necessary to develop a set of methods for predicting behavior of gliding parachutes. Gliding parachutes presented some unique problems not covered by the technology base existing in 1968. At that time a few brave jumpers were experimenting with squares. The Army was encountering difficulty in obtaining consistent performance from a small gliding system for cargo. On some days it worked; on others it did not. Engineers with parachute experience viewed the problem mainly as inconsistent deployment. Engineers with aircraft experience thought the problem was poor navigation and lack of power. Neither field of engineering was wholly appropriate.

Based on the observations that canopy opening was not too different from conventional parachutes in most critical respects and that canopies tended to glide with reasonable steadiness, we chose to concentrate first on the problem of guidance. As a first step, we worked out a graphical (manual) method of plotting trajectory points for a gliding canopy drifting with the wind while homing on a target. A visiting student helped with the manual labor. Soon we transferred the technique to a programmed calculator though graphs still had to be drawn by hand. The technique was crude, but it effectively demonstrated some key features of radial homing as applied to low-speed gliding parachutes.(1) This was our first use of "computer" simulation. Later we moved to a fancier programmable calculator with an X-Y plotter and studied more exotic guidance schemes.(2)(3)

However, as we investigated guidance schemes it became obvious that we needed more knowledge of the flight dynamics of gliding parachutes. Published test data was inadequate. A test program appeared to be too expensive and time-consuming. Also, we were not sure what parameters should be measured in testing - nor how to measure them. Thus, we began the development of analytical and computational techniques for study of all aspects of gliding canopies. This development effort has included models for study of longitudinal stability and for study of unrestricted flight in six-degrees-

STAMP Security Classification here

GOODRICK

of-freedom (6DOF) which have been verified recently by experiments.

Stability Analysis

The longitudinal stability is the key aspect determining glide performance of gliding parachute systems.(5) A balance must be achieved between the various moments so that the parachute maintains a steady glide at an angle of attack permitting useful glide velocities and returns to this angle if disturbed. The factors that determine the condition of balance or stability for a parachute are:

1. The orientation and location of lift and drag forces acting on the canopy;
2. The magnitude of material mass and its distribution (including payload mass);
3. The magnitude of entrained mass within the canopy which is offset by buoyancy in steady flight but must be included in determining the location of the system center of mass;
4. The location, magnitude and orientation of payload drag.

The parameters available which can be adjusted to achieve stability or "trim" at a desired glide condition differ significantly from those available in aircraft design. The key parameter is the aerodynamic force on the canopy. For the Parafoil canopy (Fig 1), wind tunnel data from nearly full scale canopies has been published(4) showing the variation of lift and drag components of aerodynamic force with angle of attack. A pair of empirical curves was fitted to the data to allow smooth calculation of forces at any angle of attack (Fig 2). Combined with an analysis of geometry and mass

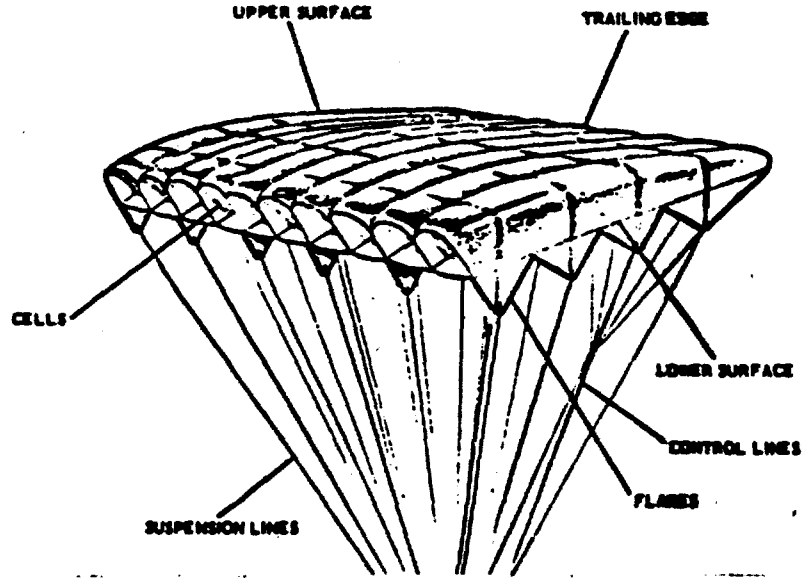

Fig 1 Parafoil Canopy

Codes
Dist | Special
A

STAMP Security Classification here

STAMP Security Classification here

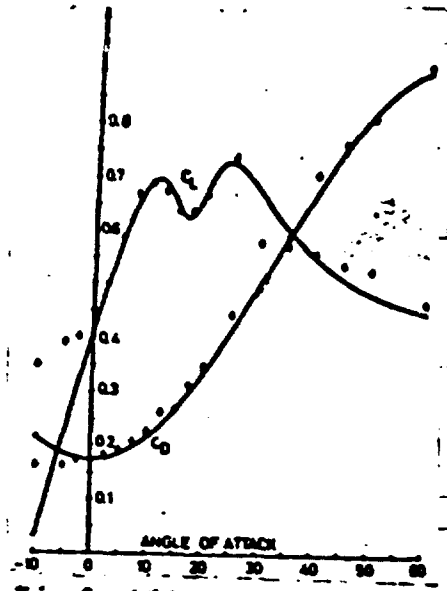

Fig 2 Lift and Drag Coefficients

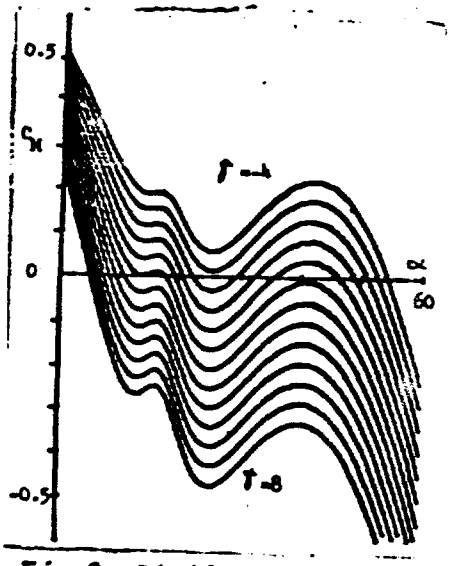

Fig 3 Static Stability (No Flap)

distribution, this permits determination of stable conditions with variation of control parameters.

There are two control parameters which may be varied independently or in combination to achieve stability. One is the angle of incidence (γ) controlled by basic suspension geometry holding the chord plane of the canopy at an angle to the axis connecting the canopy and payload centers of mass. It is convenient to define this angle as the inclination of the chordline below a line perpendicular to the axis passing between the centers of mass. For a particular setting of incidence angle, longitudinal static stability is indicated by passage of the moment coefficient (C_M) through zero with a negative slope against angle of attack (Fig 3). The second control parameter is the flap or trailing edge deflection which alters the lift and drag forces produced at any given angle of attack. Comparison of the moment coefficient variation in the two cases of zero and full flap (Fig 4) shows how variations of either or both of these parameters can affect the value of the stable angle of attack. Sport canopies are normally designed with set angles of incidence and with flap deflection varied in flight to adjust the steepness of the glide. We have tested canopies designed with variable suspension geometries for in-flight variations of angle of incidence.

The steady-state glide velocities attainable at the various stable angles of attack (following some oscillation) show that a wide range of performance is available using variable incidence (Fig 5 and 6). Optimum performance for a given canopy/payload combination can be obtained by adjustment of both control parameters.

Distance separating the payload and canopy mainly affects the steep-

STAMP Security Classification here

STAMP Security Classification here

GOODRICK

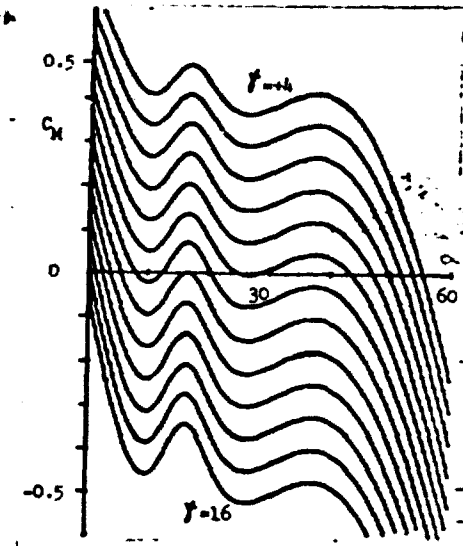

Fig 4 Static Stability (Full Flap)

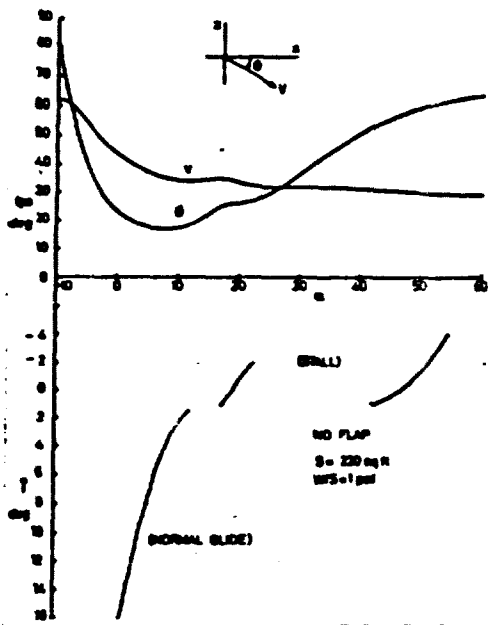

Fig 5 Range of Equilibrium Velocity (No Flap)

ness of the slope of the pitching moment with little affect on the trim angle of attack. Payload drag has a moderately significant effect. In this case a partially streamlined load is assumed.

The stability analysis has been used throughout the flight simulation studies including the 6DOF studies discussed below and has been verified in the experimental studies below. In addition to indicating the parameter settings needed to attain any desired glide performance, the stability analysis has indicated two potential problem areas requiring further study in dynamic simulations and flight tests.

1. Though larger systems have the same wing loading as small systems in order to retain similar glide velocities, canopy air mass varies as the cube of the linear scale. Thus large systems will have different static and dynamic stability which must be considered in their design.

2. Unlike aircraft which start their flight under well-controlled conditions, gliding parachutes start flying at conditions differing greatly from their design trim conditions. Hence, undesirable bistable conditions may be encountered inhibiting attainment of the desired steady glide condition unless parameters are carefully set or some means of adjustment is provided.

6DOF Simulation

A six-degree-of-freedom (6DOF) flight simulation program has evolved out of earlier, more limited simulation studies and theoretical analyses. The key features and theoretical bases of the program are discussed below. The studies using the program have yielded new information as to the nature of dynamic stability, turn control effectiveness, and effectiveness of guidance schemes. The six degrees of freedom are the three translations and the three rotations of the system of two "rigidly connected" bodies.

:rading/
:ssifi-
:n
rmation
:ret
:of
: only

STAMP Security Classification here

STAMP Security Classification here

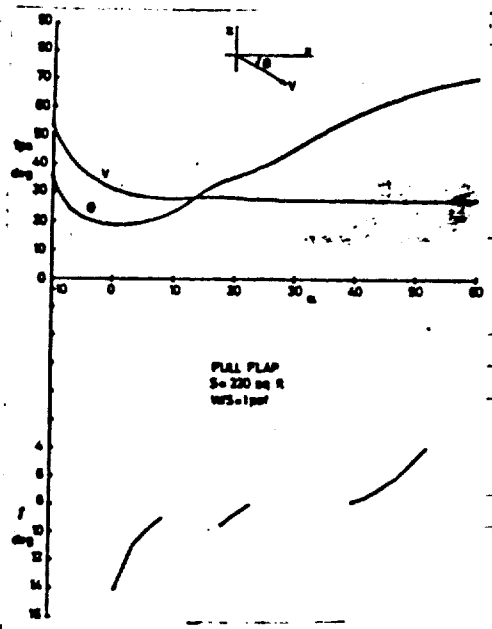

Fig 6 Range of Equilibrium Velocity (Full Flap)

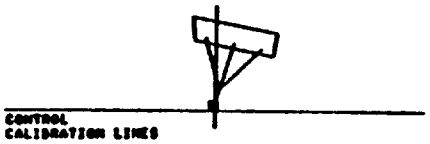

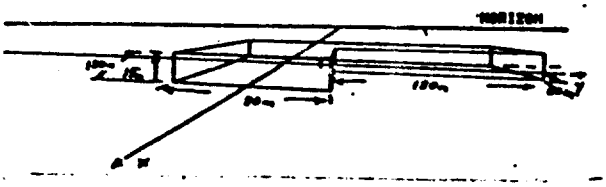

Fig 7A Simulation View from Fixed Point

Computer Program

The 6DOF simulation program for gliding parachutes features scaling functions for geometry and mass distribution, allows selection of payloads and associated drag areas, selection of variable and gusting two-dimensional wind functions, presents a deployment window plot for selection of initial conditions, features several pictorial display options during flight computation, includes a variety of manual and automatic control options, and presents plots of the parameter histories in a flexible format. A recent modification allows simulation of random errors on measured parameters used in guidance computations.

Applications of the program include study of flight mechanics and study of guidance techniques. For example, to study the turn control response of a particular canopy/payload system, calm air is selected, manual control mode is selected and a pictorial viewpoint fixed in space near the expected flight path is established. Generally, a view is selected showing a line drawing of canopy and payload relative to an inertial background (Fig 7). The display can be either a centered single image against a moving background or of multiple frozen images passing across a fixed background. The preselected type of control deflection is input via cross hairs against a calibration scale, with inputs possible at preselected intervals during the flight. The rate of change of the control deflection is controlled by a time-dependent function. The operator observes the progress, sets desired control deflections and changes the view point or format as needed. Hard copies of the display are made as required. Values of key data parameters are also displayed with the pictorial view in one of several formats. When the

STAMP Security Classification here

STAMP Security Classification here

GOODRICK

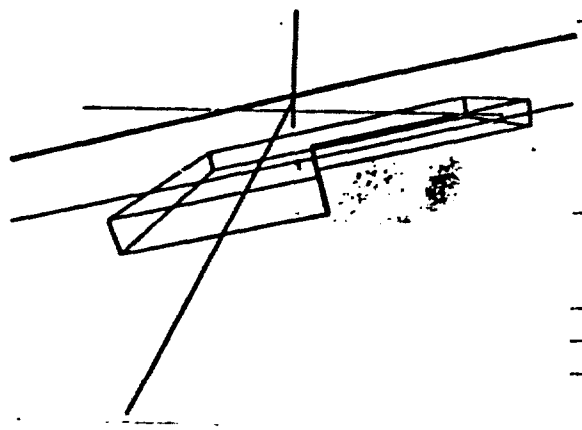

Fig 7B Simulation View from On-Board

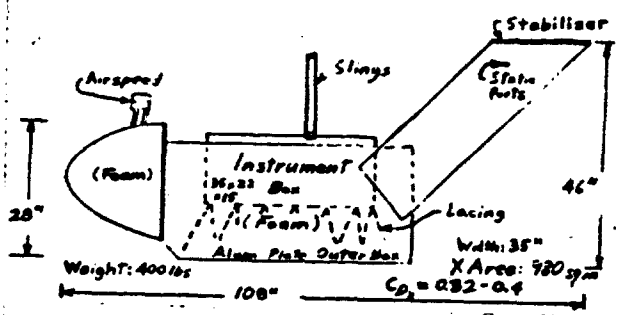

Fig 8 Flight Data Unit

maneuver is completed the operator selects the output mode in which a ground track and histories of any of 31 key parameters are plotted. The operator selects certain combinations of parameters and sets time intervals per plot.

For simulation of manual control, either an air-to-ground view from on-board the payload or a ground-to-air view from the landing zone can be selected. A variety of three-dimensional inertial references can be established. Limited data - perhaps only elapsed time - is displayed during the flight with full data available at completion. For simulation of automatic guidance, the appropriate scheme is selected and initialized if necessary. Return to manual control will occur either at a selected time or altitude. A running pictorial display is provided to monitor computer performance without delaying the computation.

Geometric and Aerodynamic Assumptions

The basic components of the program are the assumed aerodynamic and geometric characteristics and the kinematic relations. The canopy/payload system is modeled as two points connected by an inextensible line subject to tensile forces (if compressive forces occur, the payload freefalls until the orientation is such as to allow tensile forces). The payload mass contributes to system moments of inertia about the longitudinal and lateral axes only since suspension geometry usually decouples the motion about the vertical axis. A constant drag area is presently assigned to the payload although studies of particular payload configurations with lift, drag, and side forces are anticipated. The mass of the canopy is modeled as a simple rectangle inclosing an air mass. For apparent mass, up to one-half the displaced air mass (volume of air displaced by the canopy and its captive internal air) is selected as a constant added mass concentrated at the centroid in calculations of moments of inertia. The geometric distribution of the captive included air mass is considered in calculation of moments of inertia. This mass and the

STAMP Security Classification here

apparent mass change with altitude according to ambient density.

Certain unique assumptions have been made in the treatment of aerodynamic forces and moments. Empirical functions were developed for the basic wing lift and drag coefficients of Parafoil canopies measured in the wind tunnel. A side force coefficient varying with the sine of the side slip angle was also extracted from the wind tunnel data. Early attempts to incorporate these coefficients and other moment coefficients and stability derivatives measured in the wind tunnel under static conditions failed to give realistic results. Extremely low turn rates were noted under some typical quasi-steady conditions even though the data supposedly reflected the conditions of control deflection. Realistic performance - as compared with motion pictures of jumpers and limited available test data - was finally achieved by treating the canopy as geometrically distributed segments including spanwise curvature with local lift and drag computed for each segment based on local velocity and angle of attack. Local lift coefficients vary from the total wing lift coefficients in a manner approximating an elliptical distribution. The empirical functions for total wing lift and drag coefficients include effects of trailing edge deflections. To study turn and pitch (or "braking") control with trailing edge deflection, the deflection is applied via the empirical functions at selected segments. It is important to note that, due to the spanwise curvature, resultant aerodynamic forces on deflected segments may be significantly inclined to the vertical-longitudinal plane.

A study using a separate computer program was made of the quasi-static stability effects of typical velocity and angle of attack distributions resulting from the segmentation of the wing. It was found that for typical wing geometries associated with payloads from 200 to 2000 pounds, the effects of velocity distribution were highly stabilizing.(6)

Experimental Verification of Simulation

To verify the simulation program a flight test was performed using a Parafoil canopy of 200 sq ft (18.6 sq m) and a payload of 380 lbs (165 Kg) specially designed to measure those key parameters needed for verification. The emphasis of the test program was on dynamic flight conditions associated with turning maneuvers. The payload included remote radio control hardware manually activated from the ground.

Flight Data Unit

The flight data unit (FDU) serving as the payload consists of an inner box cushioned within an outer shell to which a specially shaped foam nose cone and stabilizing tail fins are attached (Fig 8). The geometry of the fins and nose cone was determined during wind tunnel tests to achieve good

static and dynamic stability. For accurate airspeed and gyro data the payload must track accurately with the canopy. The payload must also track well when carried by sling below a helicopter.

A J-Tec vortex-sensing airspeed indicator is mounted on the upper part of the nose cone. Wind tunnel tests were made for calibration at various angles of attack. Twin static ports in the surface of the vertical fins provide static pressure for the Rosemount 1241 altimeter with rate output. This mounting arrangement is not affected by moderate slideslip. The brand names of these units are mentioned because they appear to be the only units available that are adequate for this application. This was determined in several independent surveys. The J-Tec airspeed indicator acoustically senses the rate of vortex shedding from a special cross-piece in the channel of the indicator. It is highly accurate and responsive in the test range of 10 to 18 m/s. Pressure transducers would be inaccurate in this range. The Rosemount altimeter is designed for test applications with good accuracy both in altitude and electronically-derived rate measurement. Airspeed and descent rate are the two main parameters of gliding flight. Also, the horizontal component of airspeed can be calculated from the vector difference between total airspeed and descent rate only if each parameter is measured accurately.

The FDU also contains three rate gyros on the yaw, pitch and roll axes. An integrating circuit is attached to the yaw rate gyro to provide approximate heading data. The gyro data is useful in indicating the nature of turn response which can vary widely depending upon the mechanics of turn control.

Control deflection is measured from the servo potentiometers. Originally, current draw of the servo motors was measured as an indication of control force. This has been found unreliable as an indication of force because of electrical transients. Modifications are being made to measure forces from transducers linked to the lines.

A 14-channel FM tape recorder is used to record all signals. A playback unit re-transforms the FM signal to voltage analog to drive a strip-chart recorder for final copy. The tape recorder is satisfactory for recording data during a flight including extreme oscillations. However, it is not satisfactory for recording data under high-shock conditions such as during deployment and landing. Apparently, the tape is jiggled as it passes the head when the unit is jolted.

The FDU is controlled by a model aircraft radio-control system. The radio-controlled servos drive potentiometers which control the large motors drawing in control lines. Currently, two channels are used for turn and glide ratio control. Three motors and lines are used for the left turn,

right turn and glide ratio. The Parafoil is rigged for deflection of the third (or "C") flare on the second set in from each tip or turn. This produces primarily a roll tilt of the wing with a slight incidence shift. The trailing edge is separately deflected for glide control.

Weight of the payload was 355 pounds during initial testing. Later modifications added 40 pounds. This weight is carried well by the 200-square-foot Parafoil with unreefed deployment at low speeds (10-30 knots). Landing speed is somewhat high with this loading.

Except for the airspeed indicator, all equipment is housed within the inner box of the FDU (35 X 22 X 14 inches). The inner box is tied to the outer shell at the bottom and surrounded by several inches of polyurethane foam. The outer shell is 108 inches overall, including nose and tail with a cross-section of 35 X 28 inches. Drag area (C_DS) measured approximately in the wind tunnel is 2.15 - 2.69 square feet (0.2 - 0.25 sq m).

Setting System Parameters

Those aspects of the simulation model needing verification included: (1) the lift and drag functions, (2) the model resulting trim condition predicted by the longitudinal stability model, (3) the assumption that linearized moment coefficient and deviations could be replaced by local force computations at spanwise locations, and (4) the computational techniques employed. Thus, in matching flight data none of these factors were altered. Input parameters altered for the match, as listed below, were those parameters not physically measurable. Apparent mass (sometimes called "virtual" mass) is a flow field phenomenon - not a physical mass. System length depends on in-flight mass distribution and distorted suspension and canopy geometry. While these parameters could be "ballparked", they could not be physically measured. Ideally, to examine flight dynamics it is desirable to start from a steady condition. For gliding parachutes this is impossible. After over twenty flights, steady conditions have never been observed. Repeatedly, a maneuver must be entered before the efforts of a previous maneuver have dissipated even though flight appears steady from the ground. Wind turbulence adds additional disruption. The two flights matched below are the best illustrations for verification of the simulation.

To obtain a reasonable match, the following system parameters were varied in the simulation:

1. Apparent mass coefficient (one corresponds to half the volumetric displacement) was initially assumed to be 1.0. Values of 0, 0.8, 1.0, 1.5, 2.0, 3.0 were tried. Final value is 1.0!
2. Payload drag area (C_DS) was initially estimated at 0.4 sq m. Values of 0.2, 0.25, 0.3, 0.35, 0.4 were tried. Value selected is 0.2.

Wind tunnel tests later confirmed the value to be 0.20 to 0.25 sq m.

3. System length, which is the distance from payload center of mass to canopy center of mass, was varied between 5.5 m and 6.5 m. Final value is 6.5 m, which corresponds with physical measurement.

4. Trailing edge deflection was assumed and confirmed to be zero, though deflection of the edge near the tip was assumed in some trails. This method of turn control creates high initial yaw rates which were not observed in the flight data.

5. Roll-tilt turn deflection was found to be 5.0 deg in order to obtain a match. Values of 4.0 to 6.0 were tested. This parameter cannot be measured since it is the tilt angle of the resultant force vector. The flight data indicated a moderate left turn at neutral control line deflection which was matched by assuming -1.5 deg (left) tilt at neutral. Thus, in the final simulation presented here, tilt varies from -1.5 to 5.0 deg for 100% deflection.

6. Incidence coupling was found to occur with tilt-turn deflection. This was the main surprise learned in the matching process. The incidence angle is the angle of the chord below the canopy X-axis with the Z-axis passing from center of mass to payload center of mass. In the stability analysis of Reference 3, the optimum value was found to be 4 deg which appears close to the constructed value. Film of the flight test showed substantial incidence change of the section to which the control line attached. Also, it was impossible to match the characteristic initial decrease in descent rate as turn deflection was applied if incidence angle was held constant at 4 deg. But when incidence was allowed to decrease to 2 deg linearly as turn deflection went to 100%, the proper decrease in descent rate was obtained, and the proper sensitivity toward spin was observed. Though no spin occurred in the first flight, considerable sensitivity to duration of the applied stroke was observed. Thus, to obtain the data match, incidence was assumed set at 4 deg (nose down) varying to 2 deg (nose down) with 100% turn deflection.

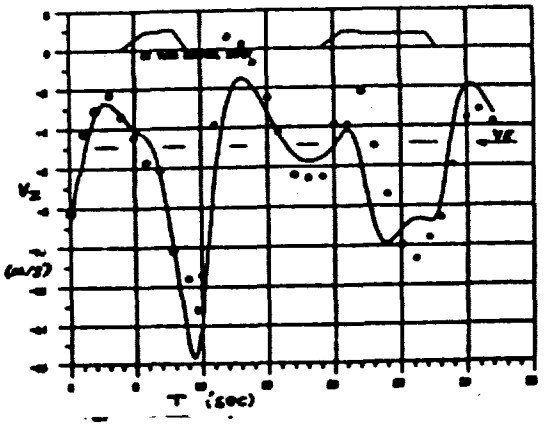

Fig 9 Descent Rate (Exp/Sim)

Comparison of Data

The descent rate data matches well in parts with certain deviations (Fig 9). Descent rate is the key parameter for comparison since all force, moment and orientation variations have a direct effect on it. Note the large deviation from equilibrium (V_Z = -4.7 m/s). This indicates that the turns are highly unsteady due to excessive deflection. Turns of moderate rate would show excursions to -6 or -7 m/s after deflection with little sensitivity to

duration of the deflection. In the simulation just previous to the one presented, the second turn deflection was a few percent greater initially, producing a peak descent rate of -16 m/s. If the first turn were held one to two seconds longer, a high rate spin would occur with descent rate peaking at -22 m/s and a turn rate of 150 deg/sec. A spin almost that bad occurred on a later flight.

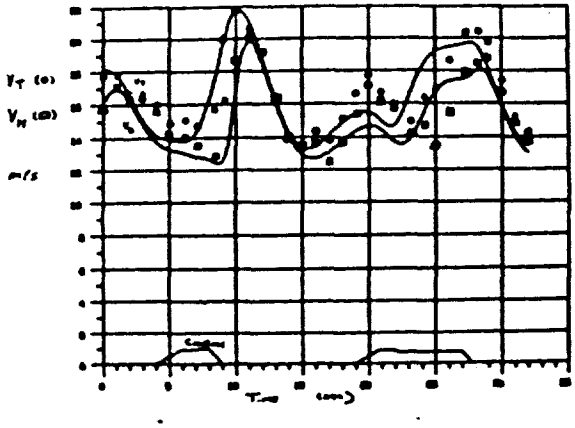

Fig 10 Total and Horizontal Airspeed

Fig 10 shows the total airspeed measured and the horizontal airspeed computed as the vector difference of total with descent rate. It was difficult to match initial conditions since the system was just recovering from a previous right turn. It is encouraging that horizontal airspeed can be accurately estimated from measurement of total airspeed and descent rate because this allows evaluation of glide performance independent of wind and also allows estimation of wind speed when compared to measured speed by a guidance system (not done for these flights).

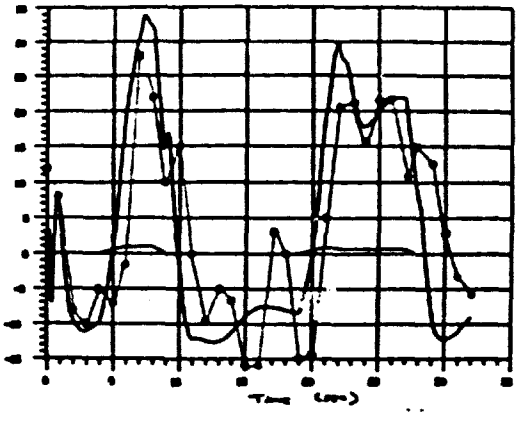

Fig 11 Yaw Rate

Fig 11 shows the axial yaw rate data. Fig 12 shows yaw, pitch and roll rates for the first turn. The gyro data includes significant "noise" caused by payload oscillations. The payload oscillations are of high rate (10 deg/sec) but of short period so that system motion can be identified. It was not known whether gyro data would be meaningful or not. For turning motions encountered in this flight there is reasonable correlation at the peaks on all axes.

Spin Performance

An unintended spin produced data which was also matched closely by simulation. During deployment, a suspension line wrapped over one cell at the tip, distorting the outer 25% of the canopy. Measured descent rate averaged 9.7 m/s with oscillations of between 0.5 and 3 m/s with a period

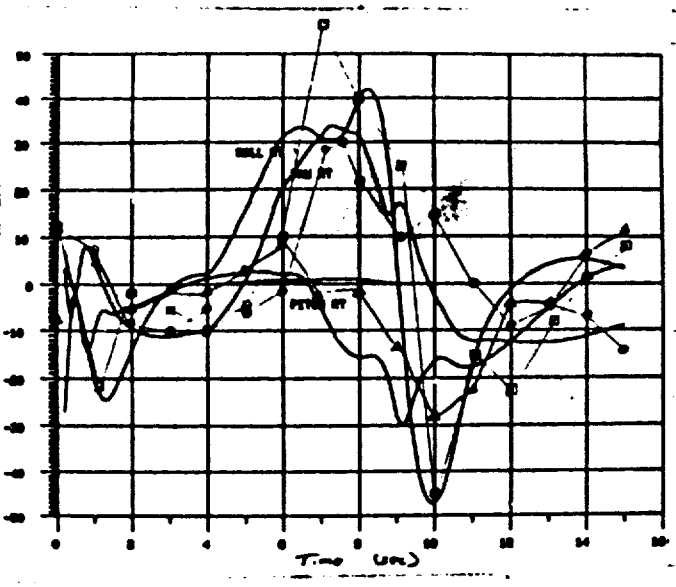

Fig 12 Rates of Yaw (O), Pitch (Δ) and Roll (□)

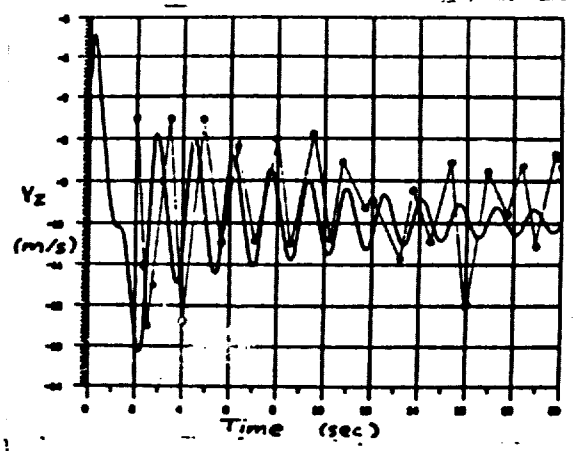

Fig 13 Descent Rate During Spin

of 1.6 seconds. Film indicated that the trailing edge was partially deflected as a result of twisted lines. Otherwise, most of the canopy was inflated to a proper shape. Simulations were made using zero, half, and full flap. Descent rates averaged 22, 10, and 8 m/s, respectively. At half flap the simulation also showed (Fig 13) an oscillation of 2 m/s, about the average of 10 m/s damping to 0.5 m/s in 11 seconds. Period of oscillation was 1.6 seconds. The Euler (or inertial) yaw rate during the flight was estimated from the video tape at 197 deg/sec (averaged over ten revolutions). Simulation at half flap indicated 205 deg/sec. Other data normally recorded was off-scale during this flight. The close match of rate of descent and yaw rate adds additional validity to the simulation model. The fact that this occurred in spite of the canopy distortion may be explained by the assumption that the distorted portion would be stalled anyway in a spin, producing only drag. Spin dynamics appear to be driven mainly by the mass distribution. The flight data did not exhibit the same damping characteristics; however, the system may have been subject to various excitations as the payload pitched, wind varied, or other changes occurred. The simulation was controlled by holding full left turn and half flap while starting at a nominal, zero-flap glide condition. The spin was established within 3 seconds. Curiously, the ground track showed tight left-turning circles whose centers precess circularly to the right.

Comparison has been made in a few other cases with results similar to those presented here. Therefore, the experimental results appear to vali-

date the simulation program as applied to a 200-square foot Parafoil of aspect ratio of 2.0 with a 350-pound payload. This conclusion is warranted because:

1. Due to the discrete character of control inputs, response is driven mainly by aerodynamic and internal properties assumed for the model.
2. The combination of multi-axial responses predicted by the model is in close agreement with experimental results.

As of this writing, about 10 good data flights have been made. The simulation model has matched salient features of most flights. There is some difficulty when wind changes occur. The data shows a response to a disturbance rather than a control input without indicating sufficient data for simulation. This has made it difficult to match flare dynamics since the few flare landings made were accompanied by some wind turbulence. The simulation has been used to identify some anomalies such as incidence shifts due to line stretch and trim change caused by a pilot chute.

Conclusion

The extent of agreement between simulation and flight data indicates that the primary factors included in the longitudinal stability analysis and in the 6DOF simulation are correct. Although the stability analysis predicts only steady-state behavior, it forms the basis required for analysis of dynamic behavior in the body-fixed XZ plane. The agreement seen in descent rate (~~Fig 9~~) would not be possible with an invalid stability model. Of course, in turning flight during the response immediately following the deflection, other factors such as the assumed spanwise distribution of lift and drag become predominant. The agreement in yaw rate (~~Fig 11~~) best illustrates correctness of this aspect of the 6DOF model. The mechanics driving motion during a spin are quite difficult to understand; however, the agreement shown in the descent rate (~~Fig 13~~) indicates that the mass ratios assumed are accurate and further justifies the assumption of spanwise distribution of lift and drag.

In further development activities on gliding parachute systems, the 6DOF model will serve to guide exploratory work and will be updated for more accurate application to different canopies and to larger systems.

References

1. Goodrick, T., "Wind Effects on Gliding Parachute Systems with Non-proportional Automatic Homing Control", TR70-28-AD, USA Natick R&D Laboratories, 1969.
2. Goodrick, T., "Estimation of Wind Effect on Gliding Parachute Cargo Systems Using Computer Simulation", Paper #70-1193, American Institute for Aeronautics and Astronautics (AIAA), 1970.

STAMP Security Classification here

3. Goodrick, T., Pearson, A., Murphy, A., "Analysis of Various Automatic Homing Techniques for Gliding Airdrop Systems with Comparative Performance in Adverse Winds", Paper #73-462, American Institute for Aeronautics and Astronautics (AIAA), 1973.

4. Ware, George M. and Hassell, Jones L. Jr., "Wind Tunnel Investigation of Ram-Air-Inflated All-Flexible Wings of Aspect Ratios 1.0 to 3.0", NASA TM SX-1923, Langly Research Center, 1969.

5. Goodrick, T., "Theoretical Study of the Longitudinal Stability of High-Performance Gliding Airdrop Systems", Paper #75-1394, American Institute for Aeronautics and Astronautics (AIAA), 1973.

6. Goodrick, T., "Simulation Studies of the Flight Dynamics of Gliding Parachute Systems", Paper #79-0417, American Institute for Aeronautics and Astronautics (AIAA), 1979.